

## FLUIDIZED BED AS A SOLID PRECURSOR DELIVERY SYSTEM IN A CHEMICAL VAPOR DEPOSITION REACTOR

Constantin Vahlas<sup>1</sup>, Brigitte Caussat<sup>2</sup>, François Senocq<sup>1</sup>, Wayne L. Gladfelter<sup>3</sup>  
Christos Sarantopoulos<sup>1</sup>, David Toro<sup>1</sup>, Tyler Moersch<sup>3</sup>

<sup>1</sup> Centre Interuniv. de Recherche et d'Ingénierie des Matériaux (CIRIMAT CNRS).  
ENSIACET, 118 route de Narbonne, F-31077 Toulouse cedex 4, France

<sup>2</sup> Laboratoire de Génie Chimique (LGC CNRS-INPT).

5 rue Paulin Talabot, BP1301, 31106 Toulouse Cedex 1, France

<sup>3</sup> Chemistry Department, University of Minnesota  
207 Pleasant St., SE, Minneapolis, MN 55455 United States

Chemical vapor deposition (CVD) using precursors that are solids at operating temperatures and pressures, presents challenges due to their relatively low vapor pressures. In addition, the sublimation rates of solid state precursors in fixed bed reactors vary with particle and bed morphology. In a recent patent application, the use of fluidized bed (FB) technology has been proposed to provide high, reliable, and reproducible flux of such precursors in CVD processes. In the present contribution, we first focus on the reactor design which must satisfy fluidization, sublimation and CVD reactor feeding constraints. Then, we report mass transport results on the sublimation of aluminium acetylacetonate, a common precursor for the CVD of alumina films. Finally, we discuss the efficiency of the precursor feeding rate, we address advantages and drawbacks of the invention and we propose design modifications in order to meet the process requirements.

## INTRODUCTION

In almost all chemical vapor deposition (CVD) processes, the precursor is either gaseous (e.g.  $\text{SiH}_4$ ) or liquid (e.g.  $\text{Ga}(\text{CH}_3)_3$ ) at ambient. Recent efforts to improve and to extend the use of such processes by designing new precursors have encountered a common problem: as the size and the complexity of the molecular precursor are increased, the state of the precursor at standard pressure and temperature becomes solid. Solid precursors are notorious for providing gas phase concentrations that are both low and that vary with time: both of which create problems in CVD processing. Moreover, actual laboratory scale solid precursor delivery systems do not achieve complete saturation of the carrier gas flowing over or through the thermoregulated particle bed (1). This situation is particularly detrimental to solid precursors with relatively low vapor pressures. For example, numerous inorganic compounds yield mass flow rates through classical delivery systems which are even lower than those thermodynamically predicted. For this among other reasons, they are used as starting compounds for the synthesis of molecular precursors which are expectedly more volatile but also more expensive.

A well known solution to this problem is to inject into the deposition zone droplets or vapors of a liquid solution containing the solid compound (2). However, such technologies present drawbacks such as reduced solubility of the precursor,

contamination of the deposits, limited application domain to mainly oxide films and the need to handle the solvents and the effluents of the process. The present paper discusses the first results on the design, the construction and the testing of a reliable solid precursor delivery system for CVD reactors based on fluidized bed (FB) technology. FBs are commonly used for improving the transport phenomena in gas-particle systems (3). In the present case, the fluidized bed is composed of either pure precursor or precursor mixed with inert powder. The bed is heated at the sublimation temperature and the fluidization gas is enriched with the precursor vapors. This gas phase enters the CVD reactor which is positioned at the exit of the FB reactor. Sublimation of aluminum triacetylacetonate  $[\text{Al}(\text{acac})_3]$  is used as a model system. This is a common, solid precursor for the CVD of alumina with low saturated vapor pressure (see for ex. (4)).

In that which follows, the characteristics of powders are presented first. Transport in a classical, though optimized, fixed bed sublimator is investigated as a reference. The principle and the design of the FB reactor are then presented, followed by a study of the fluidisability of the precursor mixtures. Finally, the flow rate of the precursor sublimed in the FB is presented, and the advantages, as well as the potential improvements of the process, are discussed.

## EXPERIMENTAL

$[\text{Al}(\text{acac})_3]$  (Acros Organics) was used as received. Its particle density is  $1.27 \text{ g/cm}^3$  and its grain size varied between  $2.3 \text{ }\mu\text{m}$  and  $35.6 \text{ }\mu\text{m}$  with a mean value  $11.6 \text{ }\mu\text{m}$ . Saturated vapor pressure is provided by the expression  $\log P(\text{kPa}) = 3.44 - 2359/T(\text{K})$  (5). Corundum powder (Baikowski) with density  $3.97 \text{ g/cm}^3$  and grain sizes between  $128 \text{ }\mu\text{m}$  and  $353 \text{ }\mu\text{m}$  and mean value  $206 \text{ }\mu\text{m}$  was used as the fluidization medium. These two powders belong to groups C and B, respectively in Geldard's classification (6). Figure 1 presents scanning electron microscopy (SEM) micrographs of both powders. Their aspect ratio is 0.93 for  $[\text{Al}(\text{acac})_3]$  and 0.68 for corundum indicating that, in agreement with the illustrated morphology, the latter presents an irregular, non-spherical shape. Pure  $\text{N}_2$  (99.999%, Air Products) was used as the carrier and fluidizing gas.

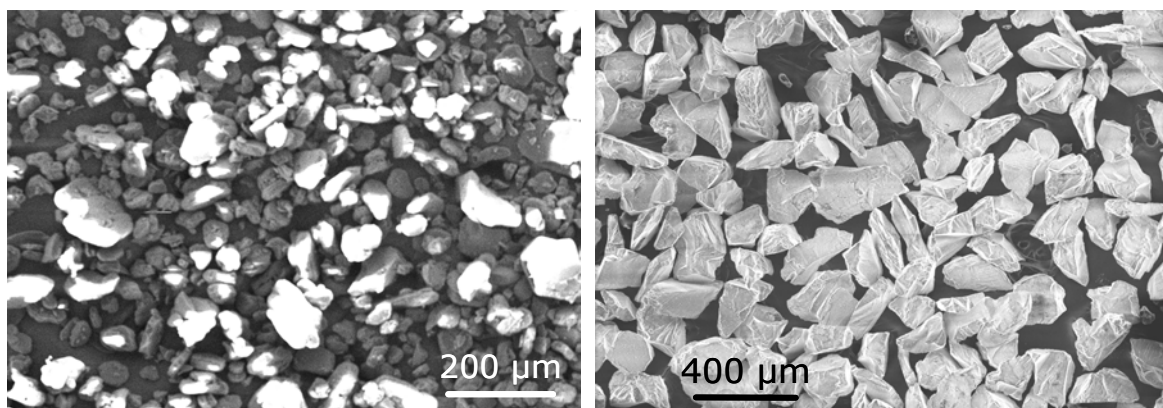


Figure 1. SEM micrographs of the  $[\text{Al}(\text{acac})_3]$  (left) and of the corundum (right) powders.

## Design of the FB reactor

Figure 2 presents the schematic of the FB reactor. It is composed of a stainless steel tube with a grid at the bottom to maintain the bed at rest. The reactor is connected at its lower part with a 6 mm  $N_2$  line and at its top with an expansion vessel to allow particles entrained by the gas flow to drop back into the bed. Both connections are made with 60 degree conical parts. The  $N_2$  line is equipped with two mass flow controllers (Brooks), one to regulate the flow rate up to the maximum desired value and the other, with lower range, for fine tuning flow rate values around the minimum fluidization velocity,  $U_{mf}$ . At the exit of the expansion vessel the saturated gas passes through a 20  $\mu m$  stainless steel filter and then through one of two parallel traps immersed in alcohol solution cooled to 243K. The traps are used to prevent release of  $[Al(acac)_3]$  into the atmosphere and also to quantify the precursor flux.

The setup is thermoregulated by heating tapes all the way from the exit of the mass flow controllers to the entrance of the traps except for the FB which is heated by a resistive furnace. The temperature of the bed is measured by a thermocouple which is immersed axially in the FB. Prior entering the FB, the  $N_2$  temperature is raised to the desired value by passing in a heated coiled copper tube.

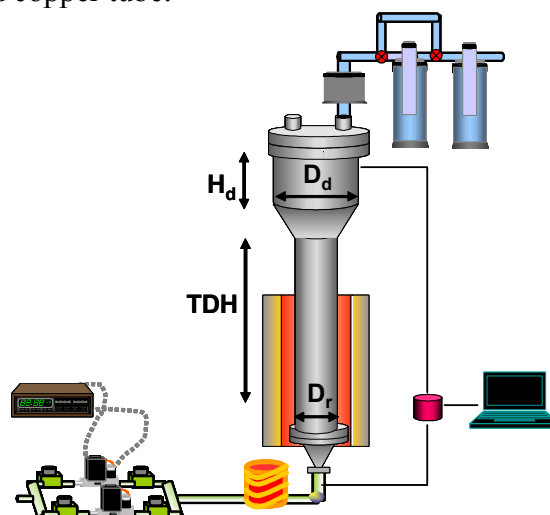


Figure 2. Schematic of the FB reactor illustrating the optimized dimensions.

Preliminary experiments allowed empirical determination of the diameter of the fluidization zone to be 53 mm. This is a standard value for stainless steel tubes; it minimizes the influence of the walls to the fluidization quality and at the same time it does not require vast quantities of the precursor and of the fluidization gas. The reactor's height was made equal to the transport disengagement height (TDH) of  $[Al(acac)_3]$ . TDH is defined as the height above which the particles flow rate is constant; it was calculated to be 910 mm taking into account a gas velocity  $U$  equal to four times  $U_{mf}$ . The diameter of the expanded freeboard section,  $D_d$  was calculated to be 250 mm for Reynolds number smaller than 0.4 and for a terminal velocity of the  $[Al(acac)_3]$  particles equal to 0.0038 m/s. The height  $H_d$  of this section was taken equal to  $D_d$ . The pressure drop  $\Delta P$  across the bed was monitored by a differential pressure transducer (GE Druck) operating in the range 0-100 torr and connected to a PC through a National Instruments card.

## RESULTS AND DISCUSSION

### Sublimation in fixed bed

Figure 3 presents the flow rate of the precursor vs.  $N_2$  flow rate through a fixed bed maintained at 393K. The schematic of the classical sublimator used for this purpose is also presented. The points on the diagram correspond to experimental results obtained with a bed of 10 g of  $[Al(acac)_3]$ . Precursor flow rate can be described by the equation :

$$Q_{pr,t} = [1 - \exp(-\beta M / Q_{carrier})] * (Q_{carrier} * P_{vap}) / P_{tot} \quad [1]$$

where  $Q_{pr,t}$  is the precursor flow rate (sccm) at time t, M is the mass of precursor in the saturator at the time t,  $Q_{carrier}$  is the carrier gas flow rate through the saturator,  $P_{vap}$  is the precursor vapour pressure at operating temperature of the saturator and  $P_{tot}$  is the overall pressure. Factor  $\beta$  has the dimension of a mass transfer coefficient. It depends on saturator geometry, on the nature and physical state of the precursor and on the operating temperature. The value of  $\beta$  is an indicator of the saturator efficiency: the higher  $\beta$  the closer  $Q_{pr,t}$  to the flow rate of a saturated gas phase. Infinite efficiency of the sublimator; i.e. for infinite value of  $\beta$  in equation [1], is illustrated in Figure 2 by the dashed straight line. In the present case,  $\beta$  was determined by mass transport measurements and was found to be equal to 205. By inputting this value in equation [1],  $Q_{pr,t}$  was estimated in the same conditions but for different values of M. The results are illustrated in Figure 2 by the different grey lines. It can be concluded that in sublimation conditions involving such a fixed bed, a large quantity of  $[Al(acac)_3]$ , namely 150 g, is necessary to approach the maximum efficiency of the process.

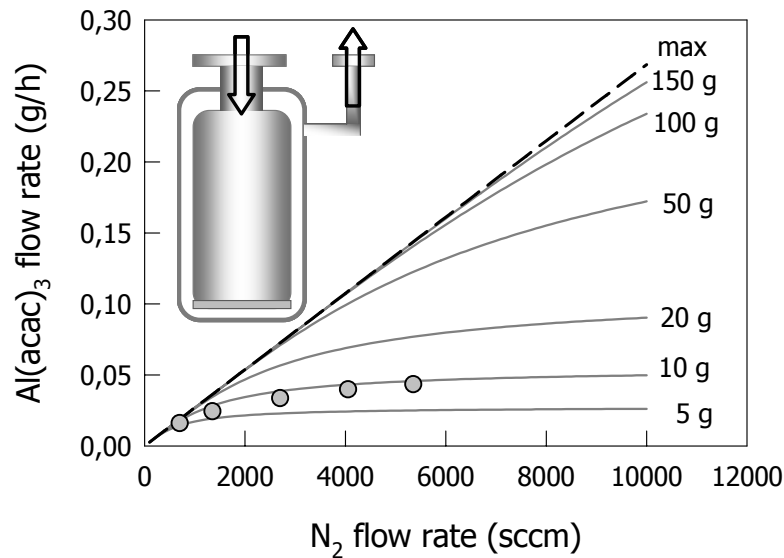


Figure 3. Schematic of a fixed bed sublimator and corresponding  $[Al(acac)_3]$  vs.  $N_2$  flow rates. Experimental results (circles), theoretical upper limit of the flow rate (dashed line) and estimated flow rates for different quantities of the precursor in the sublimator (grey lines).

## Fluidization

Figure 4 presents the differential pressure drop  $\Delta P$  vs.  $N_2$  velocity across a bed composed of corundum powders with 1.68 wt%  $[Al(acac)_3]$ . The ratio  $H/D$  corresponding to the height of the static bed over the diameter of the reactor equals 3. Both bed temperature (393K) and  $[Al(acac)_3]$  quantity (10 g) are the same as those maintained in sublimation in the fixed bed. Measurements obtained for increasing and decreasing flow rates across the bed are shown. The curves are very close; they are composed of a steep, nearly linear increase of  $\Delta P$  at low gas velocity, followed by a plateau. This behavior is characteristic of convenient fluidization, occurring in the range of gas velocities corresponding to stable values of  $\Delta P$ . From this diagram,  $U_{mf}$  can be determined at the intersection of the two regimes and was found to be equal to 0.0265 m/s. The value of  $\Delta P$  corresponding to the fluidization regime is located around 2500 Pa, while the theoretical pressure drop (dashed line) corresponding to the apparent bed weight is close to 2800 Pa. This difference is attributed to the fact that a part of the powders was found systematically either elutriated or fixed to the walls due to electrostatic forces.

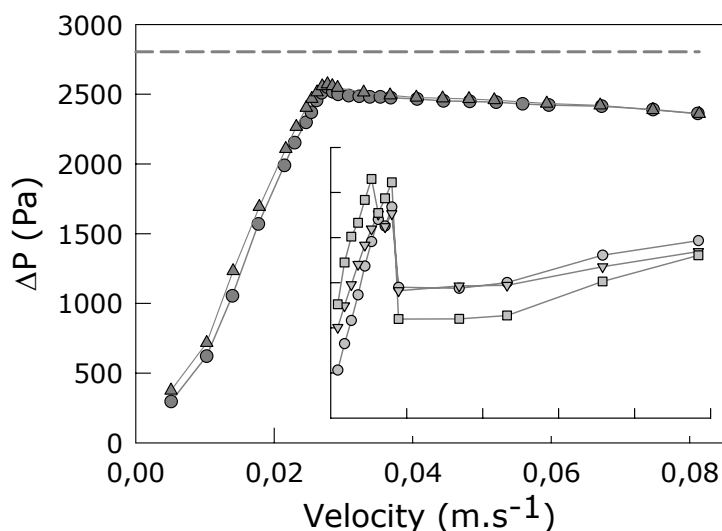


Figure 4. Differential pressure vs. gas velocity for increasing (circles) and decreasing (triangles) flow rates across a bed with  $H/D = 3$ , maintained at 393K and composed of corundum powders containing 10 g (1.68 wt%)  $[Al(acac)_3]$ . The insert is a similar diagram for three runs through a bed composed of pure  $[Al(acac)_3]$ .

Fluidization experiments in various conditions revealed that convenient fluidization is obtained for beds with  $H/D$  values between 1 and 4 (inclusive), and with  $[Al(acac)_3]$  concentration up to 10 wt%. Minor degradation of the fluidization quality was observed for beds with  $[Al(acac)_3]$  concentration of 20 wt%. Above this value, the behavior of the bed is strongly influenced by the physical characteristics of the precursor which are representative of Geldart's group C powders. Fluidization quality is poor, as illustrated by the  $\Delta P$  vs.  $N_2$  velocity diagram in the insert of Figure 4, obtained for pure  $[Al(acac)_3]$  bed. In view of these results, it is concluded that participation of an inert medium with adequate fluidization behavior is necessary for the efficient operation of the FB sublimator. This point should be considered as an advantage rather than a constraint, because the design of the reactor and its operating conditions can be now based on appropriately selected inert media for the fluidization, thus providing extended

applicability of the reactor to a series of molecular or inorganic precursors. Moreover, it appears that the involved quantity of the precursor in each run is not related to that of the bed, allowing for economic and environmentally compatible handling of the precursors.

### Sublimation in fluidized bed

Figure 5 presents the flow rate of the precursor vs.  $N_2$  flow rate and the equivalent  $U/U_{mf}$  ratio through a FB maintained at 393K. Circles and the straight line are those of figure 3; i.e. they correspond to the experimental results obtained in fixed bed and to the theoretical value of the precursor flow rate at 393K, respectively. These values were taken as a reference for comparison with the results obtained from the FB. The vertical dashed line corresponds to a gas flow rate value equal to  $U_{mf}$ . Diamonds correspond to flow rates obtained in the FB. Values are higher than the theoretical limit and this artifact is attributed to the additional sublimation of  $[Al(acac)_3]$  in zones of the reactor above the FB. Indeed, thermal regulation capabilities of this first version of the FB sublimator did not allow a tight temperature profile all along the different parts of the reactor. Consequently, in order to avoid condensation of the  $[Al(acac)_3]$  vapors in cooler parts above the FB, temperature was maintained higher than 393K, namely from 398K at the reactor above the FB up to 433K at the filter. Taking into account that some of the powders were fixed to the walls due to electrostatic forces, or elutriated up to the filter, the obtained results were attributed to precursor sublimation at a temperature higher than 393K.

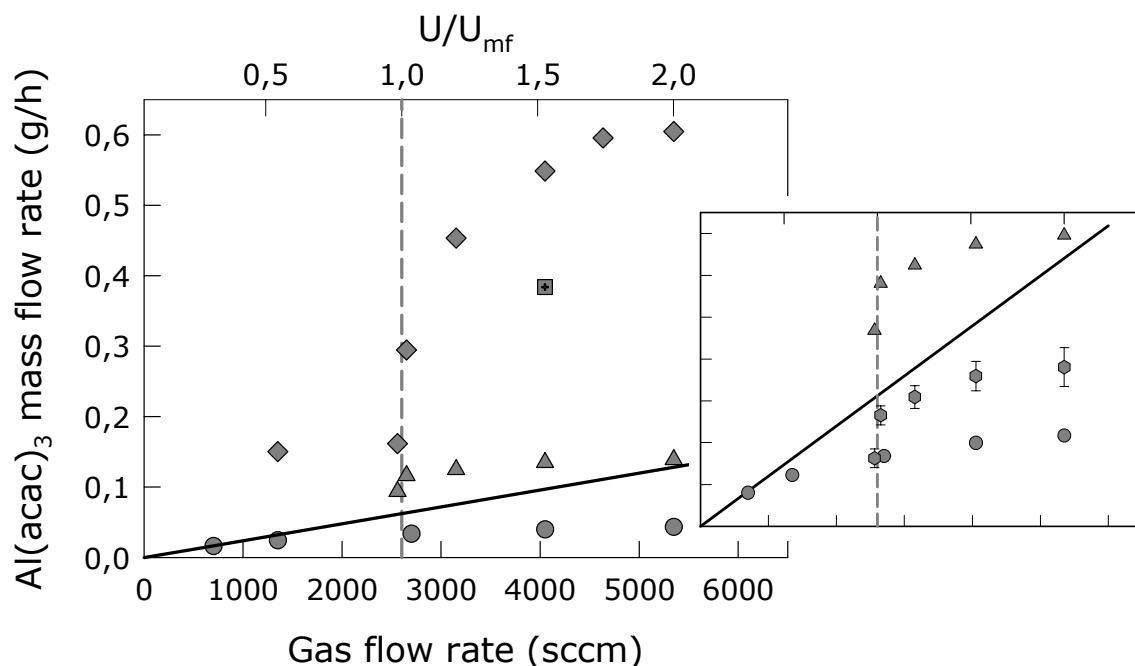


Figure 5.  $[Al(acac)_3]$  mass flow rate vs. Fluidization gas flow rate and of the equivalent  $U/U_{mf}$  ratio. Plain line: theoretical (upper limit) values at 393K. Dashed line: lower fluidization limit corresponding to  $U/U_{mf}=1$ . Circles : experimental points from fixed bed sublimator operating in the same conditions. Diamonds: experimental points from FB with thermal regulation above 393K. Square: experimental point with improved (more tight) thermal profile. Triangles: experimental points obtained with coarse  $[Al(acac)_3]$  powder. Hexagons: calculated points by subtracting from triangles the mass fraction of the powder corresponding to particles with size smaller than 20  $\mu m$ .

The square at  $U/U_{mf} = 1.5$  corresponds to  $[\text{Al}(\text{acac})_3]$  flow rate obtained by improving the thermal profile of the reactor and especially by decreasing the temperature of the filter to 405K. Although temperature excess relative to 393K is still responsible for part of the overestimation of the yield of the process, the discrepancy is also attributed to particle transportation through the filter to the trap. To verify this point, the  $[\text{Al}(\text{acac})_3]$  powder was dissolved in toluene and was recrystallized by slowly evaporating the solvent. The mean particle size was increased to 80  $\mu\text{m}$ . The results with this new powder and with the improved thermal profile of the reactor are visualized in Figure 5 by the triangles. These results are now very close, but still above the theoretical upper limit of the sublimation-controlled transport of  $[\text{Al}(\text{acac})_3]$ . This behavior is attributed to the inefficiency of filtration of particles whose size is less than that of the pores of the filter; i.e. 20  $\mu\text{m}$ . Indeed, if the weight of this fraction of particles is subtracted from the last results, the obtained values correspond to the hexagons in the insert of figure 5. There are different solutions to the problem of particles entrainment. A simple one is the use of filters with reduced porosity, such as 3  $\mu\text{m}$ . While another solution is to use screens above the FB in order to reduce particle entrainment. These two solutions have been applied in a second version of the FB sublimator which is currently under construction.

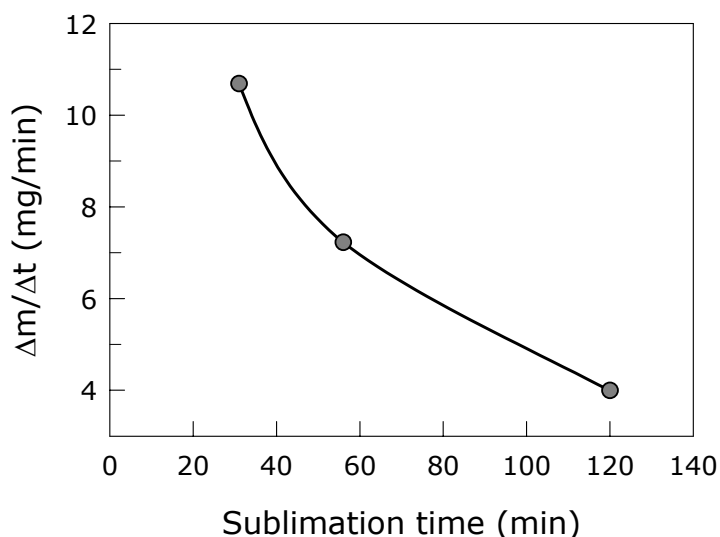


Figure 6. Evolution of the feeding rate of  $[\text{Al}(\text{acac})_3]$  in three time intervals, namely 0-30 min, 30-55 min and 55-120 min. in sublimation conditions materialized by diamonds in figure 5.

The results illustrated in figure 5 reveal that, provided the question of the entrainment of particles is solved, the performance of the FB is considerably better than that of fixed bed sublimator. However, it systematically appears that the higher the  $\text{N}_2$  flow rate, the higher the deviation of the  $[\text{Al}(\text{acac})_3]$  flow rate from the theoretical one. Although this behavior seems equivalent to that occurring during sublimation in fixed bed, it is not attributed to the same phenomenon; i.e. to the less efficient gas-solid exchange with increasing carrier gas flow rate. It is due rather to the decrease of the precursor quantity in the FB with increasing sublimation time and  $\text{N}_2$  flow rate. This is illustrated in Figure 6, which shows the evolution of the feeding rate of  $[\text{Al}(\text{acac})_3]$  in three time intervals, namely 0-30 minutes, 30-55 minutes and 55-120 minutes in sublimation conditions

materialized by diamonds in figure 5. It appears that, due to the efficiency of the sublimation process, the initial quantity of  $[\text{Al}(\text{acac})_3]$  is not enough to maintain a constant sublimation rate for long time periods in the adopted batch process. This problem can potentially be solved in FB sublimators operating with continuous feeding of the precursor, which is a technically proved solution in FB technology.

## CONCLUSIONS

We have demonstrated the use of fluidized bed technology to provide high precursor flux from solid state precursors in a consistent and controllable manner. The operating conditions and reactor geometry necessary for fluidization have been reported. Superior performance in comparison to classical sublimators has been confirmed by experiment. Particle entrainment in the gas flow caused the precursor flux to exceed theoretical values. Methods to reduce the particle loss and other improvements to increase the consistency and reliability of precursor delivery were suggested.

## ACKNOWLEDGMENTS

This work was supported by CNRS-NSF grant #14562 between CIRIMAT and the Chemistry Department of the University of Minnesota and by grants from the National Science Foundation (INT-0233328 and CHE-03159540)

## REFERENCES

1. P. O'Brien, N. L. Pickett, and D. J. Otway, *Chem. Vapor Deposition*, **8**, 237 (2002).
2. J.-P. Senateur, C. Dubourdieu, F. Weiss, M. Rosina, and A. Abrutis, *Adv. Mater. Opt. Electron.*, **10**, 155 (2000).
3. C. K. Gupta and D. Sathiyamoorthy, *Fluid bed technology in materials processing*. CRC Press, Boca Raton, FL (1999).
4. M. P. Singh and S. A. Shivashankar, *Surf. Coat. Techn.*, **161**, 135 (2002).
5. R. Theghil, D. Ferro, L. Bencivenni, and M. Pelino, *Thermochim. Acta*, **44**, 213 (1981).
6. D. Geldart, *Powder Technol.*, **7**, 285 (1973).